

ARTICLE TEMPLATE

State-of-Charge Estimation for Li-ion Batteries With Uncertain Parameters and Uncorrelated/Correlated Noises: A Recursive Approach

Junwei Wang^{a,b}, Bo Shen^{a,b}, Zidong Wang^c, Fuad E. Alsaadi^d and Khalid H. Alharbi^d

^a College of Information Science and Technology, Donghua University, Shanghai 201620, China; ^b Engineering Research Center of Digitalized Textile and Fashion Technology, Ministry of Education, Shanghai 201620, China; ^c Department of Computer Science, Brunel University London, Uxbridge, Middlesex, UB8 3PH, United Kingdom; ^d Department of Electrical and Computer Engineering, Faculty of Engineering, King Abdulaziz University, Jeddah 21589, Saudi Arabia

ARTICLE HISTORY

Compiled October 15, 2021

ABSTRACT

In this paper, the recursive state-of-charge (SOC) estimation problem is investigated for the Li-ion batteries. The uncertain parameters, which are used to account for the effects of the changing temperatures, the battery power and the drift current of current sensors, are considered in the modeling process of the Li-ion batteries. Moreover, the uncorrelated/correlated noises are also considered based on the engineering practice. The aim of the paper is to design a SOC estimation scheme such that an upper bound on the estimation error covariance is guaranteed, and such an upper bound is then minimized by appropriately designing the estimator gain. Finally, simulation experiments are carried out to demonstrate the effectiveness of our proposed SOC estimation scheme.

KEYWORDS

Correlated noises, energy and power systems, Li-ion battery, recursive estimation, state-of-charge (SOC) estimation, uncertain parameters.

1. Introduction

Recently, electric vehicles have received persistent attention due to their environment-friendly nature and zero-carbon emission (Burke, 2007; Khaligh, & Li, 2010; Xiong, Cao, Yu, He, & Sun, 2018). In order to achieve an adequate tradeoff between the endurance and the performance, Li-ion batteries have been widely used in mobile equipment, electric vehicles and aircraft. Despite the advantages such as the high energy density, low maintenance cost and a long lifetime, Li-ion batteries are sensitive to different working conditions and environment changes (Kim, Song, Son, Ono, & Qi, 2019). As a key index, the state-of-charge (SOC), which indicates the situations of the Li-ion batteries, plays a vital role in ensuring the safe usage, maximizing the performance and increasing the cycle life of the Li-ion batteries (Zhang, Hu, Wang, Sun, &

Dorrell, 2018). Unfortunately, due to the limitations of the measuring techniques, the SOC can't be measured directly. As such, there exists an urgent need to develop a state estimation scheme to estimate the SOC of Li-ion batteries.

As a key module of the battery management system, accurate yet efficient SOC estimation plays a vital role in the operation and control of electric vehicles. Up to now, there are mainly two kinds of models, named the electrochemical model and the electrical equivalent circuit model, which are used to characterize the Li-ion batteries (Xiong, Cao, Yu, He, & Sun, 2018). Although the electrochemical model is more precise, the parameter identification process of such a model is quite difficult. Compared with the electrochemical model, the electrical equivalent circuit one is more suitable for application since the tradeoff between the precision and complexity has been better achieved (Pizarro-Carmona, Cortes-Carmona, Palma-Behnke, Calderon-Munoz, Orchard, & Estevez, 2019). Specifically, the most common way of characterizing the electrical equivalent circuit model is to resort to the multi-order resistance-capacitance (RC) elements (Xiong, Cao, Yu, He, & Sun, 2018). However, as reported in Kollmeyer, Hackl, & Emadi (2017), such kind of method has difficulty in accurately revealing the dynamic behaviors of the Li-ion batteries. Fortunately, in order to overcome the drawbacks mentioned above, some improved electrical equivalent circuit models have been proposed. For example, in Andre, Meiler, Steiner, Walz, Soczka-Guth, & Sauer (2011), the Zarc element has been introduced to capture the high and low frequency characteristics of the Li-ion batteries. Moreover, the Warburg element has been considered in Schweighofer, Wegleiter, Recheis, & Fulmek (2012) to reveal the dynamic behaviors of the Li-ion batteries. In this paper, the Li-ion battery model under consideration is similar to the one proposed in Kollmeyer, Hackl, & Emadi (2017).

So far, several estimation schemes have been developed for the SOC estimation problem for Li-ion batteries, see e.g. Cheng, Lee, Liu, & Sun (2015); Jeong, Cho, Ahn, Ryu, & Lee (2014); Xing, He, Pecht, & Kwok (2014); Yang, Zhang, & Li (2015). As one of the conventional methods, the ampere-hour integral technique, which is achieved by integrating the measured current, has been widely used in the SOC estimation problems for Li-ion batteries (Jeong, Cho, Ahn, Ryu, & Lee, 2014; Yang, Zhang, & Li, 2015). However, due to the accumulated measurement errors caused by the current sensor, the estimation accuracy of such kind of method is relatively low (Chen, Fu, & Mi, 2013). Moreover, the open circuit voltage (OCV)-SOC conversion method, which is realized through look-up tables between SOC and OCV, has also been used in the SOC estimation problem for Li-ion batteries (Cheng, Lee, Liu, & Sun, 2015; Xing, He, Pecht, & Kwok, 2014). Unfortunately, the waiting time of the OCV-SOC conversion method is pretty long since the Li-ion battery needs a long time to reach a reaction equilibrium (Xing, He, Pecht, & Kwok, 2014). As such, there is a practical need to develop new SOC estimation methods for Li-ion batteries in order to respond to the ever-increasing demand for the dynamic monitoring of electric vehicles.

Owing to the iterative nature and the model-based estimation process, the Kalman-filtering-based SOC estimation schemes have been widely deployed in the monitoring of the Li-ion batteries, see e.g. Chen, Fu, & Mi (2013); Gao, Zhang, & He (2015); He, Chen, Pan, Chen, & Wang (2016); Mastali, Vazquez-Arenas, Fraser, Fowler, Afshar, & Stevens (2013); Meng, Luo, & Gao (2016); Plett (2006); Santhanagopalan, & White (2006). Since the model of the Li-ion battery is strong nonlinear, the extended Kalman filtering approach is one of the most common methods in the SOC estimation. For example, in Mastali, Vazquez-Arenas, Fraser, Fowler, Afshar, & Stevens (2013), the SOC estimation problem has been studied by using two types of Kalman filters named the extended Kalman filter (EKF) and the dual extended Kalman filter. Moreover,

in order to reduce the calculation burden of the Jacobian matrix and better handling the nonlinear terms more precisely, the unscented Kalman filtering algorithm for SOC estimation has been proposed in He, Chen, Pan, Chen, & Wang (2016); Meng, Luo, & Gao (2016). Recently, some novel algorithms have been proposed in (Charkhgard, & Farrokhi, 2010; Chemali, Kollmeyer, Preindl, & Emadi, 2018; Li, Han, Hou, Dong, & Liu, 2020; Song, Ding, Liu, & Wang, 2020; Tan, Shen, Peng, & Liu, 2020). Nevertheless, it should be pointed out that the battery parameter variations are not considered in the above-mentioned literature. In view of the actual battery situation, some factors will result in uncertainties such as the ambient temperature (Johnson, Pesaran, & Sack, 2001), the battery power (Luo, Lv, Wang, & Liu, 2011) and the drift current of current sensors (He, Liu, Zhang, & Chen, 2013). Hence, we take the uncertainty into account in this paper.

A fundamental assumption of most existing SOC estimation algorithms for Li-ion batteries is that the process and measurement noises are uncorrelated (Feng, Wang, & Zeng, 2011). However, such an assumption is quite conservative, and in many practical situations, these two noises are often correlated due to various factors such as the complex noisy environment (Song, Zhu, Zhou, & You, 2007) and the discretization of a continuous-time system (Li, 2003). The correlated noises would largely affect the estimation accuracy of the estimator and even diverge the estimated error if they are not tackled properly. As such, the estimation problems with autocorrelated noises and/or cross-correlated noises have been extensively studied, see e.g. Feng, Wang, & Zeng (2011); Fu, & Song (2008); Hu, Wang, & Gao (2013); Qu, Li, Liu, & Alsaadi (2020). Furthermore, some optimized methods have been obtained on state estimation problems under the variance constraint recently, see e.g. Hu, Wang, Liu, Jia & Williams (2020); Zhang, Hu, Liu, Yu & Liu (2019). With respect to Li-ion batteries, correlated noises are also inevitable. For example, the measured physical signals, which are transmitted by the analog-digital converters (ADCs) in electric vehicles, would be contaminated by correlated noises. Moreover, the complex electromagnetic environment of electric vehicles may also result in the phenomenon of correlated noises. Therefore, it is of great necessity to design an effective recursive SOC estimator for Li-ion batteries in the presence of correlated noises, and this constitutes another motivation of our current research.

In response to the above discussions, in this paper, we aim to investigate the SOC estimation problem for Li-ion batteries with uncertain parameters and uncorrelated/correlated noises. The fundamental challenges can be listed as follows: 1) how can we model the Li-ion battery in the presence of uncertain parameters and uncorrelated/correlated noises? 2) how can we develop the estimation scheme which is suitable for online application? and 3) how can we ensure a minimal upper-bounded estimation error covariance? As such, great efforts have been made in this paper to meet these challenges. The main contributions of this paper can be underlined as follows: 1) the SOC estimation problem is, for the first time, addressed for Li-ion batteries with uncertain parameters and uncorrelated/correlated noises; 2) an explicit model for Li-ion batteries with uncertain parameters and uncorrelated/correlated noises is proposed that caters for a more real engineering environment; and 3) the developed recursive SOC estimation algorithm is suitable for online application. Finally, simulation experiments are implemented to illustrate the effectiveness of the proposed SOC estimation scheme for Li-ion batteries.

The rest of this paper is organized as follows. In Section 2, the Li-ion battery model with uncertain parameters and uncorrelated/correlated noises is introduced, and the recursive SOC estimator structure is presented. The main results are shown

in Section 3 where the SOC estimators for Li-ion batteries with uncertain parameters and uncorrelated/correlated noises are designed, respectively. Subsequently, the upper bounds of the estimation error covariances under the uncorrelated/correlated noises are obtained and the optimal gains are solved by minimizing such upper bounds. In Section 4, simulation experiments are performed on a detailed Li-ion battery to verify the effectiveness of the developed SOC estimation scheme. The conclusion is given in Section 5.

Notations: The notations used in this paper are standard. \mathbb{R}^n denotes the n dimensional Euclidean space. M^T represents the transpose of the matrix M . M^{-1} represents the inverse of the matrix M . I_n denotes the $n \times n$ -dimensional identity matrix. $\mathbb{E}\{x\}$ stands for the expectation of the stochastic variable x . $\text{tr}(M)$ represents the trace of M . Matrices, if they are not explicitly specified, are assumed to have compatible dimensions.

2. Problem Formulation

2.1. System Model

As one of the essential indexes of a battery, the SOC, which is defined as the ratio of available and maximum capacity, has been widely used in battery health monitoring. Generally, the SOC can be acquired through the ampere-hour integral method (i.e. the time integral of the measured battery current) as follows:

$$SOC = SOC_0 + \eta \int_0^t i(t) dt \quad (1)$$

where SOC_0 represents the initial value of SOC for a battery, η is equal to $1/3600C$ with C is the maximum battery capacity and i represents the instantaneous current.

It should be pointed out that due to the massive measurement noise and accumulated measurement errors, such kind of method cannot be directly utilized to obtain the exact value of SOC (Chen, Fu, & Mi, 2013). As such, it is an effective way to use the state estimation scheme to obtain the value of SOC in the presence of massive measurement noise and accumulated measurement errors. Before proceeding further, we are going to construct a model of the battery first. Based on the modeling approach mentioned in Kollmeyer, Hackl, & Emadi (2017), the equivalent circuit model (ECM) of a battery is shown in Fig. 1, which consists of a two-order RC network, a conductor L , an internal resistance R_0 and a Warburg element Z_{wb} . R_1, R_2 and C_1, C_2 are the resistances and the capacitors of RC networks, respectively. V_1 is the voltage drop on capacitor C_1 and V_2 is the voltage drop on capacitor C_2 . V_0 is the terminal voltage. i is the current which is positive for charging the battery and negative for discharging. E_0 is the open circuit voltage of the battery.

The differences between the general multi-order RC model are that L and Z_{wb} are added, where L aims to capture the high-frequency characteristics and Z_{wb} captures the low-frequency characteristics of a battery. Z_{wb} is a constant phase element and defined as Schweighofer, Wegleiter, Recheis, & Fulmek (2012):

$$Z_{wb} = \frac{c}{\sqrt{j\omega D}} \tanh\left(\frac{l}{\sqrt{D}} \sqrt{j\omega}\right) \quad (2)$$

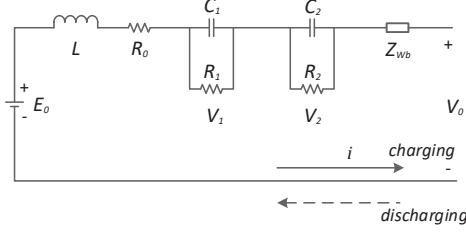


Figure 1. Equivalent circuit model of the battery.

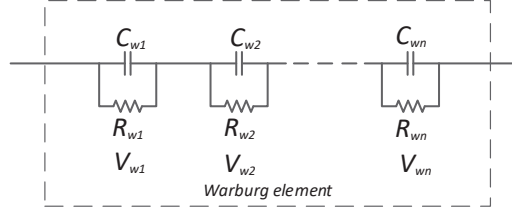


Figure 2. Equivalent model of the Warburg element as a number of RC pairs.

where ω is the angular frequency, c is a constant, D and l are the coefficient and length of diffusion, respectively. For more details about these coefficients, we refer the reader to Mauracher, & Karden (1997). For sake of the subsequent simulation program, we have to transform the Warburg element from the frequency domain to the time domain. However, such a transformation can't be executed directly due to the lack of Laplace transformation (Andre, Meiler, Steiner, Walz, Soczka-Guth, & Sauer, 2011). Fortunately, in Mauracher, & Karden (1997), an alternative method has been proposed under which the Warburg element can be equivalent to a number of RC pairs shown in Fig. 2. Therefore, the final parameters are defined as below (Mauracher, & Karden, 1997):

$$\begin{aligned}
 R_{wb} &= \frac{cl}{D}, & C_{wb} &= \frac{l}{2c}, \\
 R_{wn} &= \omega_n R_{wb}, & C_{wn} &= C_{wb}, \\
 \omega_n &= \frac{8}{(2n-1)^2 \pi^2}
 \end{aligned}$$

where n is the number of RC elements, R_{wn} , C_{wn} and ω_n are the resistance, capacitance and scaling factor of the n -th RC network, respectively. The voltage drop of the n -th RC element is defined as V_{wn} . For the tradeoff between the computational burden and accuracy of battery modeling, in this paper, we choose $n = 5$ to model the Warburg element (Kollmeyer, Hackl, & Emadi, 2017).

Next, the state space model is constructed to estimate the SOC of the battery. In this paper, we choose the voltage drop V_1 , V_2 , V_{w1} , V_{w2} , V_{w3} , V_{w4} , V_{w5} and SOC as state variables, To be specific, we can define the state vector as

$$x = [V_1, V_2, V_{w1}, V_{w2}, V_{w3}, V_{w4}, V_{w5}, SOC]^T$$

$$\triangleq [x_1, x_2, x_3, x_4, x_5, x_6, x_7, x_8]^T \in \mathbb{R}^N (N = 8).$$

In the light of Kirchhoff's current laws and (1)-(2), we can obtain the following formulas:

$$\begin{aligned} \dot{x}_1 &= -\frac{1}{R_1 C_1} x_1 + \frac{1}{C_1} i, \\ \dot{x}_2 &= -\frac{1}{R_2 C_2} x_2 + \frac{1}{C_2} i, \\ \dot{x}_3 &= -\frac{1}{R_{w3} C_{w3}} x_3 + \frac{1}{C_{w3}} i = -\frac{\pi^2}{8R_{wb} C_{wb}} x_3 + \frac{1}{C_{wb}} i, \\ \dot{x}_4 &= -\frac{1}{R_{w4} C_{w4}} x_4 + \frac{1}{C_{w4}} i = -\frac{(3\pi)^2}{8R_{wb} C_{wb}} x_4 + \frac{1}{C_{wb}} i, \\ \dot{x}_5 &= -\frac{1}{R_{w5} C_{w5}} x_5 + \frac{1}{C_{w5}} i = -\frac{(5\pi)^2}{8R_{wb} C_{wb}} x_5 + \frac{1}{C_{wb}} i, \\ \dot{x}_6 &= -\frac{1}{R_{w6} C_{w6}} x_6 + \frac{1}{C_{w6}} i = -\frac{(7\pi)^2}{8R_{wb} C_{wb}} x_6 + \frac{1}{C_{wb}} i, \\ \dot{x}_7 &= -\frac{1}{R_{w7} C_{w7}} x_7 + \frac{1}{C_{w7}} i = -\frac{(9\pi)^2}{8R_{wb} C_{wb}} x_7 + \frac{1}{C_{wb}} i, \\ \dot{x}_8 &= \eta i. \end{aligned} \tag{3}$$

Based on the above equations, the state space equation can be written into a standard form:

$$\dot{x} = Ax + Bi \tag{4}$$

where

$$A = \begin{bmatrix} -\frac{1}{R_1 C_1} & 0 & 0 & 0 & 0 & 0 & 0 & 0 \\ 0 & -\frac{1}{R_2 C_2} & 0 & 0 & 0 & 0 & 0 & 0 \\ 0 & 0 & -\frac{\pi^2}{8R_{wb} C_{wb}} & 0 & 0 & 0 & 0 & 0 \\ 0 & 0 & 0 & -\frac{(3\pi)^2}{8R_{wb} C_{wb}} & 0 & 0 & 0 & 0 \\ 0 & 0 & 0 & 0 & -\frac{(5\pi)^2}{8R_{wb} C_{wb}} & 0 & 0 & 0 \\ 0 & 0 & 0 & 0 & 0 & -\frac{(7\pi)^2}{8R_{wb} C_{wb}} & 0 & 0 \\ 0 & 0 & 0 & 0 & 0 & 0 & -\frac{(9\pi)^2}{8R_{wb} C_{wb}} & 0 \\ 0 & 0 & 0 & 0 & 0 & 0 & 0 & 0 \end{bmatrix},$$

$$B = \left[\frac{1}{C_1} \frac{1}{C_2} \frac{1}{C_{wb}} \frac{1}{C_{wb}} \frac{1}{C_{wb}} \frac{1}{C_{wb}} \frac{1}{C_{wb}} \frac{1}{C_{wb}} \eta \right]^T.$$

Discretizing the system (4) with a period T , we obtain the discretized model as follows:

$$x_{k+1} = A_d x_k + B_d i_k \tag{5}$$

where $A_d = e^{AT}$, $B_d = (\int_0^T e^{At} dt) B$.

Considering the changes of susceptible battery parameters with the factors such as the ambient temperatures, the battery power and the drift current of current sensors, the real-valued uncertain matrix ΔA_k is added to model the uncertainties. Moreover, taking the process noise into consideration, we can obtain the following equation:

$$x_{k+1} = (A_d + \Delta A_k)x_k + B_d i_k + w_k \quad (6)$$

where w_k is the process noise.

The original value of state x_0 is assumed to be a stochastic variable with:

$$\begin{aligned} \mathbb{E}\{x_0\} &= \bar{x}_0, \\ \mathbb{E}\{(x_0 - \bar{x}_0)(x_0 - \bar{x}_0)^T\} &= P_{0|0}. \end{aligned}$$

The uncertainty ΔA_k is assumed to satisfy

$$\begin{aligned} \Delta A_k &= M_k F_k N_k, \\ F_k F_k^T &\leq I_8 \end{aligned} \quad (7)$$

where F_k denotes the time-varying uncertainty, M_k and N_k are known matrices of suitable dimensions. I_8 is the identity matrix.

Remark 1. The Li-ion battery can be modeled as (3) based on the Kirchhoff's current laws and internal features of batteries. Then, the model can be written into a general continuous-time linear form (4). For the sake of estimator design and application, the continuous-time linear system (4) can be discretized as a discrete-time one as shown in (5). Since the battery parameters are easily impacted by internal or external factors, the uncertainty of battery parameters is considered in this paper. Therefore, the discretized model (5) can be further modeled as (6) by taking the parameter uncertainties and the process noise into consideration.

Remark 2. Note that the parameters of Li-ion batteries are often influenced due to the external environment changes and the internal characteristics. For example, Johnson, Pesaran, & Sack (2001) has pointed out that the internal resistance will increase when the ambient temperature is low. Moreover, the connections between the impedance parameters and the low power during the discharge cycle have also been revealed in Luo, Lv, Wang, & Liu (2011). Furthermore, He, Liu, Zhang, & Chen (2013) has also pointed out that the drift currents of the current sensor are unavoidable during the acquisition process, which may also result in the uncertain parameters. As such, the parameter uncertainty is considered in this paper.

2.2. Measurement Model

In this paper, the battery terminal voltage is chosen as the measured output since it can be obtained directly by using the voltage sensors. Note that the voltage drop of the inductor L can be neglected in a short time. As such, according to the Kirchhoff's voltage laws, the terminal voltage V_0 can be written as

$$V_0 = V_1 + V_2 + V_{w1} + V_{w2} + V_{w3} + V_{w4} + V_{w5} + E_0 + iR_0. \quad (8)$$

With the aid of curve fitting method, the open circuit voltage E_0 can be modeled as:

$$\begin{aligned} E_0 &= f(SOC) \\ &= a_1 SOC^6 + a_2 SOC^5 + a_3 SOC^4 + a_4 SOC^3 \\ &\quad + a_5 SOC^2 + a_6 SOC + a_7 \end{aligned}$$

where a_1 to a_7 are the coefficients obtained by the least square method. For more details, please refer to Section 4.1.

By letting $z = V_0$ and taking the measurement noise into consideration, the discretized version of (8) with the discrete period T can be described as

$$z_k = h(x_k) + i_k R_0 + v_k \quad (9)$$

where

$$h(x_k) = x_{1,k} + x_{2,k} + x_{3,k} + x_{4,k} + x_{5,k} + x_{6,k} + x_{7,k} + f(x_{8,k}),$$

and v_k is the measurement noise.

2.3. Cases with Correlated and Uncorrelated Noises

In order to cater for the engineering practice, the cases with correlated and uncorrelated noises are both considered in this paper.

Caes 1. Uncorrelated noises

In this case, the process noise w_k is assumed to be a Gaussian white noise with zero-mean and covariance $Q_k > 0$. Similarly, the measurement noise v_k is also assumed to be a Gaussian white noise with zero-mean and covariance $R_k > 0$. Moreover, w_k , v_k and the initial variables x_0 are mutually independent.

Caes 2. Correlated noises

In this case, the noise signals w_k and v_k have the following statistical properties:

$$\begin{aligned} \mathbb{E}\{w_k\} &= 0, \\ \mathbb{E}\{w_k w_l^T\} &= Q_k \delta_{k,l} + Q_{k,l} \delta_{k,l-1} + Q_{k,l} \delta_{k,l+1}, \\ \mathbb{E}\{v_k\} &= 0, \\ \mathbb{E}\{v_k v_l^T\} &= R_k \delta_{k,l} + R_{k,l} \delta_{k,l-1} + R_{k,l} \delta_{k,l+1}, \end{aligned} \quad (10)$$

where $Q_k > 0$, $Q_{k,l}$, $R_k > 0$ and $R_{k,l}$ are known matrices with appropriate dimensions. $\delta_{k,l}$ is the Kronecker function

$$\delta_{k,l} = \begin{cases} 1 & \text{if } k = l \\ 0 & \text{if } k \neq l. \end{cases}$$

Moreover, the signals w_k , v_k , x_0 are assumed to be mutually unrelated.

Remark 3. In case 1, the process noise and the measurement noise are both assumed to be uncorrelated. However, in practical engineering, such an assumption is fairly conservative. For example, the correlated noises are often encountered in many practical situations such as the discretisation process of a continuous-time system (Li, 2003) and the synchronisation process of the non-uniform data (Song, Zhu, Zhou, & You, 2007). Moreover, the complicated noisy environment and the applications of ADCs may also result in the correlated noises (Feng, Wang, & Zeng, 2013). As such, in case 2, the autocorrelated noises are considered.

2.4. State Estimator Structure

Based on the Li-ion battery model mentioned above, the following state estimator is constructed:

$$\begin{aligned}\hat{x}_{k+1|k} &= A_d \hat{x}_{k|k} + B_d i_k, \\ \hat{x}_{k+1|k+1} &= \hat{x}_{k+1|k} + K_{k+1} [z_{k+1} - (h(\hat{x}_{k+1|k}) + i_{k+1} R_0)]\end{aligned}\quad (11)$$

where $\hat{x}_{k+1|k}$ and $x_{k+1|k+1}$ are the one-step prediction and the estimate of state x_{k+1} , respectively, and K_{k+1} is the gain of estimator.

Substituting (9) into (11) yields

$$\begin{aligned}\hat{x}_{k+1|k+1} &= \hat{x}_{k+1|k} + K_{k+1} [(h(x_{k+1}) + i_{k+1} R_0 + v_{k+1}) - (h(\hat{x}_{k+1|k}) + i_{k+1} R_0)] \\ &= \hat{x}_{k+1|k} + K_{k+1} [h(x_{k+1}) + v_{k+1} - h(\hat{x}_{k+1|k})].\end{aligned}\quad (12)$$

Expanding $h(x_{k+1})$ around $\hat{x}_{k+1|k}$ with the aid of Taylor series expansion, we have

$$h(x_{k+1|k}) = h(\hat{x}_{k+1|k}) + H_{k+1} \tilde{x}_{k+1|k} + o(|\tilde{x}_{k+1|k}|) \quad (13)$$

where

$$H_{k+1} \triangleq (\partial h(x_{k+1}) / \partial x_{k+1})|_{x_{k+1} = \hat{x}_{k+1|k}}$$

and $o(|\tilde{x}_{k+1|k}|)$ represents the high-order terms of the Taylor series expansion which is neglected in this paper.

Combining (12) and (13), we can rewrite $x_{k+1|k+1}$ as

$$\hat{x}_{k+1|k+1} = \hat{x}_{k+1|k} + K_{k+1} (H_{k+1} \tilde{x}_{k+1|k} + v_{k+1}). \quad (14)$$

Let us define the one-step prediction error and the estimation error as follows:

$$\begin{aligned}\tilde{x}_{k+1|k} &\triangleq x_{k+1} - \hat{x}_{k+1|k}, \\ \tilde{x}_{k+1|k+1} &\triangleq x_{k+1} - \hat{x}_{k+1|k+1}.\end{aligned}\quad (15)$$

Then, it follows from (6), (9) and (11)-(15), we have

$$\begin{aligned}\tilde{x}_{k+1|k} &= A_d \tilde{x}_{k|k} + \Delta A_k x_k + w_k, \\ \tilde{x}_{k+1|k+1} &= x_{k+1} - \hat{x}_{k+1|k+1} - K_{k+1} (H_{k+1} \tilde{x}_{k+1|k} + v_{k+1}) \\ &= \tilde{x}_{k+1|k} - K_{k+1} (H_{k+1} \tilde{x}_{k+1|k} + v_{k+1})\end{aligned}\quad (16)$$

$$= (I - K_{k+1}H_{k+1})\tilde{x}_{k+1|k} - K_{k+1}v_{k+1}. \quad (17)$$

Define the one-step prediction error covariance and the estimation error covariance as $P_{k+1|k} \triangleq \mathbb{E}\{\tilde{x}_{k+1|k}\tilde{x}_{k+1|k}^T\}$ and $P_{k+1|k+1} \triangleq \mathbb{E}\{\tilde{x}_{k+1|k+1}\tilde{x}_{k+1|k+1}^T\}$, respectively. For the sake of clarity, in the case of uncorrelated noises, we use $P_{u,k+1|k}$ and $P_{u,k+1|k+1}$ to represent the one-step prediction error covariance and the estimation error covariance, and $P_{c,k+1|k}$ and $P_{c,k+1|k+1}$ are the ones in the case of correlated noises.

The aim of this paper is to design state estimation schemes for the SOC estimation under the foregoing two cases such that

- (1) the upper bounds of the estimation error covariances $\Xi_{u,k+1|k+1}$ and $\Xi_{c,k+1|k+1}$ ($\Xi_{u,k+1|k+1}$ is in the case of uncorrelated noises and $\Xi_{c,k+1|k+1}$ is in the case of correlated noises) must be guaranteed, i.e.,

$$\begin{aligned} P_{u,k+1|k+1} &\leq \Xi_{u,k+1|k+1}, \\ P_{c,k+1|k+1} &\leq \Xi_{c,k+1|k+1}. \end{aligned}$$

- (2) the upper bounds should be minimized by utilizing appropriate estimator gains $K_{u,k+1}$ and $K_{c,k+1}$ ($K_{u,k+1}$ is in the case of uncorrelated noises and $K_{c,k+1}$ is in the case of correlated noises) at each time step through a recursive method.

3. Main Results

In this section, we aim to study the SOC estimation problem with uncertain parameters under the cases of uncorrelated noises and correlated noises. In each case, the one-step prediction error covariance and the estimation error covariance are firstly characterized. Then, the upper bounds of these covariances are derived based on the stochastic analysis technique. Finally, the estimator gains are obtained by minimizing the upper bound of the estimation error covariance, respectively.

For deriving main results, we introduce the following useful lemmas.

Lemma 3.1. *For x and y are the two vectors with any dimension and γ is a positive scalar. We have*

$$x^T y + y^T x \leq \gamma x^T x + \gamma^{-1} y^T y.$$

Lemma 3.2. *For matrices M , N , X and P with appropriate dimensions, the following equations hold*

$$\begin{aligned} \frac{\partial \text{tr}(MXN)}{\partial X} &= M^T N^T, \quad \frac{\partial \text{tr}(MX^T N)}{\partial X} = NM, \\ \frac{\partial \text{tr}((MXN)P(MXN)^T)}{\partial X} &= 2M^T M X N P N^T. \end{aligned}$$

3.1. Design of The Estimator With Uncorrelated Noises

Taking (16) and (17) into account, we can obtain the recursion forms of the one-step prediction error covariance and the estimation error covariance in the case of uncorrelated noises which will be shown in the following lemma.

Lemma 3.3. *The one-step prediction error covariance $P_{u,k+1|k}$ and the estimation error covariance $P_{u,k+1|k+1}$ can be obtained as follows:*

$$\begin{aligned} P_{u,k+1|k} &= A_d P_{u,k|k} A_d^T + A_d \mathbb{E}\{\tilde{x}_{k|k} x_k^T\} \Delta A_k^T + \Delta A_k \mathbb{E}\{x_k \tilde{x}_{k|k}^T\} A_d^T \\ &\quad + \Delta A_k \mathbb{E}\{x_k x_k^T\} \Delta A_k^T + Q_k \end{aligned} \quad (18)$$

and

$$\begin{aligned} P_{u,k+1|k+1} &= (I - K_{u,k+1} H_{k+1}) P_{u,k+1|k} (I - K_{u,k+1} H_{k+1})^T \\ &\quad + K_{u,k+1} R_{k+1} K_{u,k+1}^T. \end{aligned} \quad (19)$$

Proof. Based on the definitions of one-step prediction error covariance and estimation error covariance, the validations (18) and (19) can be derived directly. Thus, the proof is omitted here for brevity. \square

Theorem 3.4. *Consider the one-step prediction error covariance $P_{u,k+1|k}$ and the estimation error covariance $P_{u,k+1|k+1}$ in (18) and (19). Let $\gamma_{1,k}$ and $\gamma_{2,k}$ be the positive scalars. If the following two Riccati-like difference equations*

$$\begin{aligned} \Xi_{u,k+1|k} &= (1 + \gamma_{2,k}) A_d \Xi_{u,k|k} A_d^T + (1 + \gamma_{2,k}^{-1}) \times \text{tr}\{N_k[(1 + \gamma_{1,k}) \Xi_{u,k|k} \\ &\quad + (1 + \gamma_{1,k}^{-1}) \hat{x}_{k|k} \hat{x}_{k|k}^T] N_k^T\} M_k M_k^T + Q_k, \end{aligned}$$

and

$$\begin{aligned} \Xi_{u,k+1|k+1} &= (I - K_{u,k+1} H_{k+1}) \Xi_{u,k+1|k} (I - K_{u,k+1} H_{k+1})^T + K_{u,k+1} R_{k+1} K_{u,k+1}^T \end{aligned}$$

with the initial condition $P_{u,0|0} \leq \Xi_{u,0|0}$ have the positive-definite solutions $\Xi_{u,k+1|k}$ and $\Xi_{u,k+1|k+1}$, then $\Xi_{u,k+1|k+1}$ is an upper bound of $P_{u,k+1|k+1}$, i.e., $P_{u,k+1|k+1} \leq \Xi_{u,k+1|k+1}$.

Moreover, such an upper bound can be minimized with the following estimator gain:

$$K_{u,k+1} = \Xi_{u,k+1|k} H_{k+1}^T (H_{k+1} \Xi_{u,k+1|k} H_{k+1}^T + R_{k+1})^{-1}. \quad (20)$$

Proof. To begin with, let us handle the first term of right-hand side of (18). By applying Lemma 3.1 and (15), we have

$$\begin{aligned} &\mathbb{E}\{x_k x_k^T\} \\ &= \mathbb{E}\{(\tilde{x}_{k|k} + \hat{x}_{k|k})(\tilde{x}_{k|k} + \hat{x}_{k|k})^T\} \leq (1 + \gamma_{1,k}) P_{u,k|k} + (1 + \gamma_{1,k}^{-1}) \hat{x}_{k|k} \hat{x}_{k|k}^T \end{aligned} \quad (21)$$

where $\gamma_{1,k}$ is a positive scalar.

Similarly, the second and third terms of the right-hand side of (18) can be tackled as

$$\begin{aligned} &A_d \mathbb{E}\{\tilde{x}_{k|k} x_k^T\} \Delta A_k^T + \Delta A_k \mathbb{E}\{x_k \tilde{x}_{k|k}^T\} A_d^T \\ &\leq \gamma_{2,k} A_d P_{u,k|k} A_d^T + \gamma_{2,k}^{-1} \Delta A_k \mathbb{E}\{x_k x_k^T\} \Delta A_k^T \end{aligned}$$

where $\gamma_{2,k}$ is a positive scalar.

Next, according to (7) and (21), we have

$$\begin{aligned} & \Delta A_k \mathbb{E}\{x_k x_k^T\} \Delta A_k^T \\ & \leq M_k F_k N_k [(1 + \gamma_{1,k}) P_{u,k|k} + (1 + \gamma_{1,k}^{-1}) \hat{x}_{k|k} \hat{x}_{k|k}^T] N_k^T F_k^T M_k^T \\ & \leq \text{tr}\{N_k [(1 + \gamma_{1,k}) P_{u,k|k} + (1 + \gamma_{1,k}^{-1}) \hat{x}_{k|k} \hat{x}_{k|k}^T] N_k^T\} M_k M_k^T. \end{aligned}$$

Then we can obtain the following inequality:

$$\begin{aligned} P_{u,k+1|k} & \leq (1 + \gamma_{2,k}) A_d P_{u,k|k} A_d^T + (1 + \gamma_{2,k}^{-1}) \text{tr}\{N_k [(1 + \gamma_{1,k}) P_{u,k|k} \\ & \quad + (1 + \gamma_{1,k}^{-1}) \hat{x}_{k|k} \hat{x}_{k|k}^T] N_k^T\} M_k M_k^T + Q_k \\ & \leq (1 + \gamma_{2,k}) A_d \Xi_{u,k|k} A_d^T + (1 + \gamma_{2,k}^{-1}) \text{tr}\{N_k [(1 + \gamma_{1,k}) \Xi_{u,k|k} \\ & \quad + (1 + \gamma_{1,k}^{-1}) \hat{x}_{k|k} \hat{x}_{k|k}^T] N_k^T\} M_k M_k^T + Q_k \end{aligned}$$

In virtue of mathematical induction, we can obtain that $P_{u,k+1|k} \leq \Xi_{u,k+1|k}$. Moreover, based on the above discussions, the following inequality can be derived

$$\begin{aligned} & P_{u,k+1|k+1} \\ & = (I - K_{u,k+1} H_{k+1}) P_{u,k+1|k} (I - K_{u,k+1} H_{k+1})^T + K_{u,k+1} R_{k+1} K_{u,k+1}^T \\ & \leq (I - K_{u,k+1} H_{k+1}) \Xi_{u,k+1|k} (I - K_{u,k+1} H_{k+1})^T + K_{u,k+1} R_{k+1} K_{u,k+1}^T. \end{aligned}$$

By using the mathematical induction approach, it is not difficult to verify that

$$P_{u,k+1|k+1} \leq \Xi_{u,k+1|k+1}.$$

Finally, we are ready to derive the estimator gain by minimizing the upper bound $\Xi_{u,k+1|k+1}$. According to Lemma 3.2, taking the partial derivative of $\Xi_{u,k+1|k+1}$ with respect to $K_{u,k+1}$ and letting the derivative be zero, we have

$$\begin{aligned} & \frac{\partial \text{tr}(\Xi_{u,k+1|k+1})}{\partial K_{u,k+1}} \\ & = -2(I - K_{u,k+1} H_{k+1}) \Xi_{u,k+1|k} H_{k+1}^T + 2K_{u,k+1} R_{k+1} \\ & = 0. \end{aligned} \tag{22}$$

Based on (22), the estimator gain can be determined as the form shown in (20). Therefore, the proof of this theorem is complete. \square

Up to now, the upper bound of the estimator error covariance has been obtained in the presence of uncertain parameters and such an upper bound has been minimized by appropriately designing an estimator gain. It is worth noting that the developed state estimation scheme can be applied to the dynamic state estimation for SOC due to its iterative nature. In the following, the impacts of the correlated noises are considered.

3.2. Design of The Estimator With Correlated Noises

In this subsection, the correlated noises with properties (10) are considered. The one-step prediction error covariance and the estimation error covariance are firstly shown

in the following lemmas.

Lemma 3.5. *Taking the impacts of the correlated noises into consideration, the one-step prediction error covariance $P_{c,k+1|k}$ can be described as*

$$\begin{aligned}
P_{c,k+1|k} &= A_d P_{c,k|k} A_d^T + A_d \mathbb{E}\{\tilde{x}_{k|k} x_k^T\} \Delta A_k^T + \Delta A_k \mathbb{E}\{x_k \tilde{x}_{k|k}^T\} A_d^T \\
&\quad + A_d (Q_{k-1,k} - K_{c,k} H_k Q_{k-1,k}) + (Q_{k-1,k} - K_{c,k} H_k Q_{k-1,k})^T A_d^T \\
&\quad + \Delta A_k \mathbb{E}\{x_k x_k^T\} \Delta A_k^T + \Delta A_k Q_{k-1,k} + Q_{k-1,k}^T \Delta A_k^T + Q_k.
\end{aligned} \tag{23}$$

Proof. From (16), the one-step prediction error covariance is obtained as follows:

$$\begin{aligned}
P_{c,k+1|k} &= \mathbb{E}\{\tilde{x}_{k+1|k} \tilde{x}_{k+1|k}^T\} \\
&= A_d P_{c,k|k} A_d^T + A_d \mathbb{E}\{\tilde{x}_{k|k} x_k^T\} \Delta A_k^T + \Delta A_k \mathbb{E}\{x_k \tilde{x}_{k|k}^T\} A_d^T \\
&\quad + A_d \mathbb{E}\{\tilde{x}_{k|k} w_k^T\} + \mathbb{E}\{w_k \tilde{x}_{k|k}^T\} A_d^T + \Delta A_k \mathbb{E}\{x_k x_k^T\} \Delta A_k^T \\
&\quad + \Delta A_k \mathbb{E}\{x_k w_k^T\} + \mathbb{E}\{w_k x_k^T\} \Delta A_k^T + \mathbb{E}\{w_k w_k^T\}.
\end{aligned} \tag{24}$$

Noting (10), we can derive that

$$\begin{aligned}
\mathbb{E}\{x_k w_k^T\} &= \mathbb{E}\{[(A_d + \Delta A_{k-1})x_{k-1} + B_d i_{k-1} + w_{k-1}] w_k^T\} \\
&= Q_{k-1,k}.
\end{aligned} \tag{25}$$

Moreover, by applying (6), (10), (14) and (25), the term $\mathbb{E}\{\tilde{x}_{k|k} w_k^T\}$ can be derived as follows:

$$\begin{aligned}
\mathbb{E}\{\tilde{x}_{k|k} w_k^T\} &= \mathbb{E}\{x_k w_k^T\} - \mathbb{E}\{\hat{x}_{k|k} w_k^T\} \\
&= Q_{k-1,k} - \mathbb{E}\{[\hat{x}_{k|k-1} + K_{c,k}(z_k - h(\hat{x}_{k|k-1}) - R_0 i_{k-1})] w_k^T\} \\
&= Q_{k-1,k} - \mathbb{E}\{[\hat{x}_{k|k-1} + K_{c,k}(H_k \tilde{x}_{k|k-1} + v_k)] w_k^T\} \\
&= Q_{k-1,k} - (I - K_{c,k} H_k) \mathbb{E}\{\hat{x}_{k|k-1} w_k^T\} - K_{c,k} \mathbb{E}\{(H_k x_k + v_k) w_k^T\} \\
&= Q_{k-1,k} - K_{c,k} H_k \mathbb{E}\{x_k w_k^T\} - K_{c,k} \mathbb{E}\{v_k w_k^T\} \\
&= Q_{k-1,k} - K_{c,k} H_k Q_{k-1,k}.
\end{aligned} \tag{26}$$

By noting that $\hat{x}_{k|k-1}$ and v_k are uncorrelated with the noise w_k , the term $\mathbb{E}\{\hat{x}_{k|k-1} w_k^T\}$ and $\mathbb{E}\{v_k w_k^T\}$ equal to zero when deriving (26). It follows from (24)-(26) that (23) holds, which completes the proof. \square

Lemma 3.6. *The estimation error covariance $P_{c,k+1|k+1}$ in this situation can be written as follows:*

$$\begin{aligned}
&P_{c,k+1|k+1} \\
&= (I - K_{c,k+1} H_{k+1}) P_{c,k+1|k} (I - K_{c,k+1} H_{k+1})^T + (I - K_{c,k+1} H_{k+1}) A_d K_{c,k} R_{k,k+1} \\
&\quad \times K_{c,k+1}^T + K_{c,k+1} R_{k,k+1}^T K_{c,k}^T A_d^T (I - K_{c,k+1} H_{k+1})^T + K_{c,k+1} R_{k+1} K_{c,k+1}^T.
\end{aligned} \tag{27}$$

Proof. From (17), the estimation error covariance $P_{c,k+1|k+1}$ can be obtained as

$$\begin{aligned}
& P_{c,k+1|k+1} \\
&= \mathbb{E}\{\tilde{x}_{k+1|k+1}\tilde{x}_{k+1|k+1}^T\} \\
&= (I - K_{c,k+1}H_{k+1})P_{c,k+1|k}(I - K_{c,k+1}H_{k+1})^T - (I - K_{c,k+1}H_{k+1})\mathbb{E}\{\tilde{x}_{k+1|k}v_{k+1}^T\} \\
&\quad \times K_{c,k+1}^T - K_{c,k+1}\mathbb{E}\{v_{k+1}\tilde{x}_{k+1|k}^T\}(I - K_{c,k+1}H_{k+1})^T + K_{c,k+1}\mathbb{E}\{v_{k+1}v_{k+1}^T\}K_{c,k+1}^T.
\end{aligned} \tag{28}$$

The term $\mathbb{E}\{\tilde{x}_{k+1|k}v_{k+1}^T\}$ in (28) can be derived as follows:

$$\mathbb{E}\{\tilde{x}_{k+1|k}v_{k+1}^T\} = \mathbb{E}\{x_{k+1}v_{k+1}^T\} - \mathbb{E}\{\hat{x}_{k+1|k}v_{k+1}^T\}$$

where

$$\begin{aligned}
\mathbb{E}\{x_{k+1}v_{k+1}^T\} &= \mathbb{E}\{[(A_d + \Delta A_k)x_k + B_d i_k + w_k]v_{k+1}^T\} \\
&= 0
\end{aligned} \tag{29}$$

and

$$\begin{aligned}
& \mathbb{E}\{\hat{x}_{k+1|k}v_{k+1}^T\} \\
&= \mathbb{E}\{(A_d\hat{x}_{k|k} + B_d i_k)v_{k+1}^T\} \\
&= \mathbb{E}\{A_d[\hat{x}_{k|k-1} + K_{c,k}(z_k - h(\hat{x}_{k|k-1}) - R_0 i_{k-1})]v_{k+1}^T + B_d i_k v_{k+1}^T\} \\
&= \mathbb{E}\{A_d[\hat{x}_{k|k-1} + K_{c,k}(H_k \tilde{x}_{k|k-1} + v_k)]v_{k+1}^T + B_d i_k v_{k+1}^T\} \\
&= A_d(I - K_{c,k}H_k)\mathbb{E}\{\hat{x}_{k|k-1}v_{k+1}^T\} + A_d K_{c,k}H_k\mathbb{E}\{x_k v_{k+1}^T\} + A_d K_{c,k}\mathbb{E}\{v_k v_{k+1}^T\} \\
&= A_d K_{c,k}R_{k,k+1}.
\end{aligned} \tag{30}$$

By noting that $\hat{x}_{k|k-1}$ and x_k are uncorrelated with v_{k+1} , the term $\mathbb{E}\{\hat{x}_{k|k-1}v_{k+1}^T\}$ and $\mathbb{E}\{x_k v_{k+1}^T\}$ equal to zero when deriving (30). It follows from (28)-(30) that (27) holds, which completes the proof. \square

Theorem 3.7. Consider the one-step prediction error covariance $P_{c,k+1|k}$ and the estimation error covariance $P_{c,k+1|k+1}$ in (23) and (27). Let $\gamma_{3,k}$, $\gamma_{4,k}$ and $\gamma_{5,k}$ be the positive scalars. If the following two Riccati-like difference equations

$$\begin{aligned}
& \Xi_{c,k+1|k} \\
&= (1 + \gamma_{4,k})A_d\Xi_{c,k|k}A_d^T + (1 + \gamma_{4,k}^{-1})tr\{N_k\Theta_k N_k^T\}M_k M_k^T + \gamma_{5,k}N_k N_k^T M_k M_k^T \\
&\quad + \gamma_{5,k}^{-1}Q_{k-1,k}Q_{k-1,k}^T + A_d(Q_{k-1,k} - K_{c,k}H_k Q_{k-1,k}) \\
&\quad + (Q_{k-1,k} - K_{c,k}H_k Q_{k-1,k})^T A_d^T + Q_k
\end{aligned}$$

and

$$\begin{aligned}
& \Xi_{c,k+1|k+1} \\
&= (I - K_{c,k+1}H_{k+1})\Xi_{c,k+1|k}(I - K_{c,k+1}H_{k+1})^T + (I - K_{c,k+1}H_{k+1})A_d K_{c,k}R_{k,k+1}
\end{aligned}$$

$$\times K_{c,k+1}^T + K_{c,k+1} R_{k,k+1}^T K_{c,k}^T A_d^T (I - K_{c,k+1} H_{k+1})^T + K_{c,k+1} R_{k+1} K_{c,k+1}^T,$$

with the initial condition $P_{c,0|0} \leq \Xi_{c,0|0}$ have the positive-definite solutions $\Xi_{c,k+1|k}$ and $\Xi_{c,k+1|k+1}$ where

$$\Theta_k = (1 + \gamma_{3,k}) \Xi_{c,k|k} + (1 + \gamma_{3,k}^{-1}) \hat{x}_{k|k} \hat{x}_{k|k}^T,$$

then, the matrix $\Xi_{c,k+1|k+1}$ is the upper bound of $P_{c,k+1|k+1}$, namely

$$P_{c,k+1|k+1} \leq \Xi_{c,k+1|k+1}.$$

Moreover, such an upper bound can be minimized at each time step through the following estimator gain:

$$K_{c,k+1} = (H_{k+1} \Xi_{c,k+1|k} - R_{k,k+1}^T K_{c,k}^T A_d^T) \Omega_{k+1}^{-1} \quad (31)$$

where

$$\begin{aligned} \Omega_{k+1} &= H_{k+1} \Xi_{c,k+1|k} H_{k+1}^T - H_{k+1} A_d K_{c,k} R_{k,k+1} \\ &\quad - R_{k,k+1}^T K_{c,k}^T A_d^T H_{k+1}^T + R_{k+1}. \end{aligned}$$

Proof. Let's consider the right side of (23) term by term. Based on Lemma 3.1 and (15), the term $\mathbb{E}\{x_k x_k^T\}$ can be tackled as

$$\begin{aligned} &\mathbb{E}\{x_k x_k^T\} \\ &= \mathbb{E}\{(\tilde{x}_{k|k} + \hat{x}_{k|k})(\tilde{x}_{k|k} + \hat{x}_{k|k})^T\} \leq (1 + \gamma_{3,k}) P_{c,k|k} + (1 + \gamma_{3,k}^{-1}) \hat{x}_{k|k} \hat{x}_{k|k}^T. \end{aligned} \quad (32)$$

Similarly, the second and third terms of the right side of (23) can be rearranged as

$$\begin{aligned} &A_d \mathbb{E}\{\tilde{x}_{k|k} x_k^T\} \Delta A_k^T + \Delta A_k \mathbb{E}\{x_k \tilde{x}_{k|k}^T\} A_d^T \\ &\leq \gamma_{4,k} A_d P_{c,k|k} A_d^T + \gamma_{4,k}^{-1} \Delta A_k \mathbb{E}\{x_k x_k^T\} \Delta A_k^T. \end{aligned}$$

Moreover, the seventh and eighth terms of the right side of (32) can be written as follows:

$$\Delta A_k Q_{k-1,k}^T + Q_{k-1,k} \Delta A_k^T \leq \gamma_{5,k} \Delta A_k \Delta A_k^T + \gamma_{5,k}^{-1} Q_{k-1,k} Q_{k-1,k}^T.$$

Noting that (7) and (32), we can obtain the following two inequalities:

$$\begin{aligned} &\Delta A_k \Delta A_k^T \\ &= M_k F_k N_k N_k^T F_k^T M_k^T \leq N_k N_k^T M_k M_k^T \end{aligned}$$

and

$$\begin{aligned} &\Delta A_k \mathbb{E}\{x_k x_k^T\} \Delta A_k^T \\ &\leq M_k F_k N_k [(1 + \gamma_{3,k}) P_{c,k|k} + (1 + \gamma_{3,k}^{-1}) \hat{x}_{k|k} \hat{x}_{k|k}^T] N_k^T F_k^T M_k^T \\ &\leq \text{tr}\{N_k [(1 + \gamma_{3,k}) P_{c,k|k} + (1 + \gamma_{3,k}^{-1}) \hat{x}_{k|k} \hat{x}_{k|k}^T] N_k^T\} M_k M_k^T. \end{aligned}$$

Based on the above discussions, we have

$$\begin{aligned}
& P_{c,k+1|k} \\
& \leq (1 + \gamma_{4,k})A_d P_{c,k|k} A_d^T + (1 + \gamma_{4,k}^{-1})tr\{N_k[(1 + \gamma_{3,k})P_{c,k|k} + (1 + \gamma_{3,k}^{-1})\hat{x}_{k|k}\hat{x}_{k|k}^T]N_k^T\} \\
& \quad + \gamma_{5,k}N_k N_k^T M_k M_k^T + \gamma_{5,k}^{-1}Q_{k-1,k}Q_{k-1,k}^T + A_d(Q_{k-1,k} - K_{c,k}H_k Q_{k-1,k}) \\
& \quad + (Q_{k-1,k} - K_{c,k}H_k Q_{k-1,k})^T A_d^T + Q_k \\
& \leq (1 + \gamma_{4,k})A_d \Xi_{c,k|k} A_d^T + (1 + \gamma_{4,k}^{-1})tr\{N_k[(1 + \gamma_{3,k})\Xi_{c,k|k} + (1 + \gamma_{3,k}^{-1})\hat{x}_{k|k}\hat{x}_{k|k}^T]N_k^T\} \\
& \quad + \gamma_{5,k}N_k N_k^T M_k M_k^T + \gamma_{5,k}^{-1}Q_{k-1,k}Q_{k-1,k}^T + A_d(Q_{k-1,k} - K_{c,k}H_k Q_{k-1,k}) \\
& \quad + (Q_{k-1,k} - K_{c,k}H_k Q_{k-1,k})^T A_d^T + Q_k.
\end{aligned} \tag{33}$$

In virtue of mathematical induction, it is not difficult to verify that $P_{c,k+1|k} \leq \Xi_{c,k+1|k}$.

Based on Lemma 3.6 and (33), we have

$$\begin{aligned}
& P_{c,k+1|k+1} \\
& = (I - K_{c,k+1}H_{k+1})P_{c,k+1|k}(I - K_{c,k+1}H_{k+1}^T) + (I - K_{c,k+1}H_{k+1})A_d K_{c,k} R_{k,k+1} K_{c,k+1}^T \\
& \quad + K_{c,k+1} R_{k,k+1}^T K_{c,k}^T A_d^T (I - K_{c,k+1}H_{k+1})^T + K_{c,k+1} R_{k+1} K_{c,k+1}^T \\
& \leq (I - K_{c,k+1}H_{k+1})\Xi_{c,k+1|k}(I - K_{c,k+1}H_{k+1}^T) + (I - K_{c,k+1}H_{k+1})A_d K_{c,k} R_{k,k+1} K_{c,k+1}^T \\
& \quad + K_{c,k+1} R_{k,k+1}^T K_{c,k}^T A_d^T (I - K_{c,k+1}H_{k+1})^T + K_{c,k+1} R_{k+1} K_{c,k+1}^T.
\end{aligned}$$

In the light of the mathematical induction approach, we can conclude that

$$P_{c,k+1|k+1} \leq \Xi_{c,k+1|k+1}.$$

Now, we are ready to solve the estimator gain by minimizing the upper bound $\Xi_{c,k+1|k+1}$. Taking the partial derivative of the upper bound $\Xi_{c,k+1|k+1}$ with respect to $K_{c,k+1}$ and letting the result be zero, we have

$$\begin{aligned}
& \frac{\partial tr(\Xi_{c,k+1|k+1})}{\partial K_{c,k+1}} \\
& = -2(I - K_{c,k+1}H_{k+1})\Xi_{c,k+1|k}H_{k+1}^T + 2K_{c,k+1}R_{k+1} + 2A_d K_{c,k} R_{k,k+1} \\
& \quad - 2K_{c,k+1}H_{k+1}A_d K_{c,k} R_{k,k+1} - 2K_{c,k+1}R_{k,k+1}^T K_{c,k}^T A_d^T H_{k+1}^T \\
& = 0.
\end{aligned}$$

Based on the above equation, the estimator gain $K_{c,k+1}$ is obtained as the form shown in (31). The proof is complete. \square

So far, we have designed the recursive estimation scheme to estimate SOC of batteries. The designed state estimators will be validated in the next section in the experiments and simulations of a detailed battery.

Remark 4. Until now, the SOC estimation problem has been studied for Li-ion batteries with uncertain parameters and uncorrelated/correlated noises. Based on the Kirchhoff's laws and internal features of batteries, the Li-ion batteries with uncertain parameters and uncorrelated/correlated noises are modeled in (6) and (9) and the

state estimator is constructed in (11). It should be noted that the exact value of the one-step prediction error covariance can't be obtained directly due to the presence of the uncertainty matrix ΔA_k . Hence, it is impossible to obtain the exact value of the estimation error covariance. In order to sort out this problem, the upper bounds of the one-step prediction error covariance as well as the estimation error covariance are obtained in Theorem 3.4 and Theorem 3.7. Then, the upper bounds of the estimation error covariances are minimized by appropriately designing the estimator gain.

4. Simulation Results

In this section, the parameter identification of a Li-ion battery is performed firstly. Then, simulation experiments under two cases are carried out to test our proposed SOC estimation scheme. Moreover, the comparisons between the standard EKF and our proposed estimation method are also presented.

4.1. Battery Parameter Extraction

The battery data set can be obtained by testing a Panasonic NCR18650PF Li-ion battery, which is used in Tesla's electric vehicles (Kollmeyer, 2018).

To identify the parameters of the battery, the Electrochemical Impedance Spectroscopy (EIS) tests, which is a general method of analyzing the electric double layer and diffusion of the electrode process by measuring the changes of the impedance with the frequency changing sine wave, are carried out in 25 °C (Andre, Meiler, Steiner, Walz, Soczka-Guth, & Sauer, 2011). The experimental fitting model is sufficient to fit the battery performance since it can cover the frequency from 1 kHz to 100 mHz. The measured EIS curve and the fitted curve at 25 °C are shown in Fig. 3.

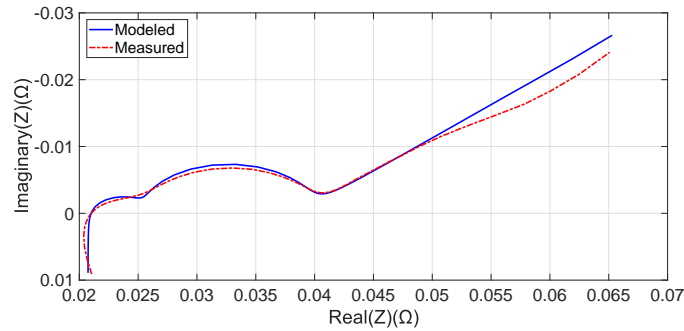


Figure 3. The fitting result to EIS measurement at 25 degree.

According to the least square method, the obtained parameters of the battery model at a temperature of 25 °C are shown in Table 1.

Table 1. The parameter values of Li-ion batteries

Parameter	Value
L	$2.47 \times 10^{-7} H$
R_0	0.0207Ω
R_1	0.0034Ω
C_1	$0.1676 F$
R_2	0.0042Ω
C_2	$1.9570 F$
R_{wb}	0.1894Ω
C_{wb}	$1084 F$

In accordance with (5), the system parameters are

$$A_d = \begin{bmatrix} 2.1580 \times 10^{-76} & 0 & 0 & 0 & 0 & 0 & 0 & 0 \\ 0 & 5.2922 \times 10^{-6} & 0 & 0 & 0 & 0 & 0 & 0 \\ 0 & 0 & 0.9940 & 0 & 0 & 0 & 0 & 0 \\ 0 & 0 & 0 & 0.9474 & 0 & 0 & 0 & 0 \\ 0 & 0 & 0 & 0 & 0.9704 & 0 & 0 & 0 \\ 0 & 0 & 0 & 0 & 0 & 0.9588 & 0 & 0 \\ 0 & 0 & 0 & 0 & 0 & 0 & 0.9474 & 0 \\ 0 & 0 & 0 & 0 & 0 & 0 & 0 & 1 \end{bmatrix},$$

$$B_d = \begin{bmatrix} 0.0034 \\ 0.0042 \\ 9.1974 \times 10^{-4} \\ 3.0475 \times 10^{-4} \\ 1.8176 \times 10^{-4} \\ 1.2905 \times 10^{-4} \\ 9.9779 \times 10^{-5} \\ 9.5785 \times 10^{-6} \end{bmatrix}.$$

The parameters of the uncertainty ΔA_k are set as $F_k = 0.2\sin(k)$, $M_k = [0.1 \ 0.1 \ 0.1 \ 0.1 \ 0.1 \ 0.1 \ 0.1 \ 0.0001]^T$ and $N_k = [1 \ 1 \ 1 \ 1 \ 1 \ 1 \ 1 \ 0.001]$.

Since the OCV is a function of the SOC, we can obtain the OCV-SOC curve by performing the Hybrid PulsePower Characteristic (HPPC) test (Kollmeyer, Hackl, & Emadi, 2017). Fig. 4a shows the mean squared error (MSE) of various polynomials which are used to fit the OCV-SOC curve.

From Fig. 4a, we can find that the six-order polynomial equation can achieve a tradeoff between the accuracy of fitting and the computational burden. Therefore, as shown in Fig. 4b, the six-order polynomial equation is used to fit the OCV-SOC curve. To be more specific, the expression of the OCV-SOC curve is given by:

$$E_0 = 12.1428SOC^6 - 33.3722SOC^5 + 30.7913SOC^4 - 8.1766SOC^3 - 2.6534SOC^2 + 2.3112SOC + 3.1322.$$

4.2. Battery SOC Estimation

In this part, the pulse current test is carried out on the MATLAB/Simulink firstly. Experiments consist of a series of the constant pulse which lasts for 140s and then returns to 0 for 1860s. The pulse current is a typical 1 C rate (i.e. 2.9 A). The plots of the input current and battery terminal voltage are shown in Fig. 5. Moreover,

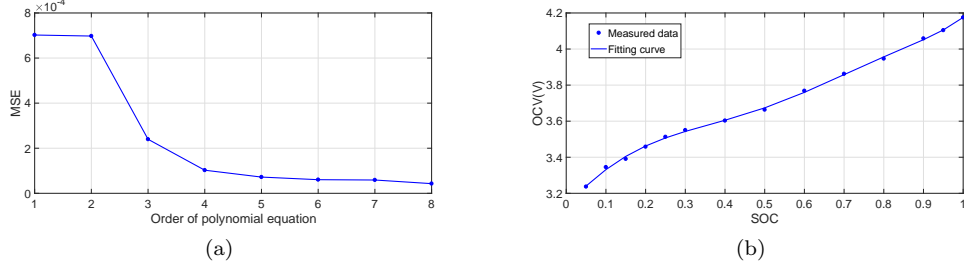


Figure 4. (a) The MSE of different polynomial orders. (b) The OCV-SOC curve.

the current and terminal voltages under the Urban Dynamometer Driving Schedule (UDDS) are shown in Fig. 6 (Kollmeyer, Hackl, & Emadi, 2017).

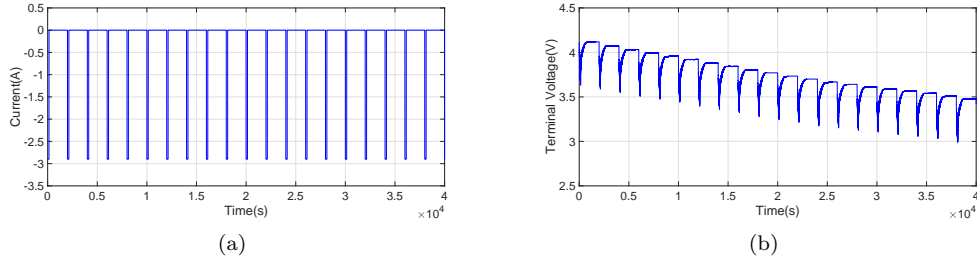


Figure 5. Pulse current test. (a) Discharging current. (b) Terminal voltage.

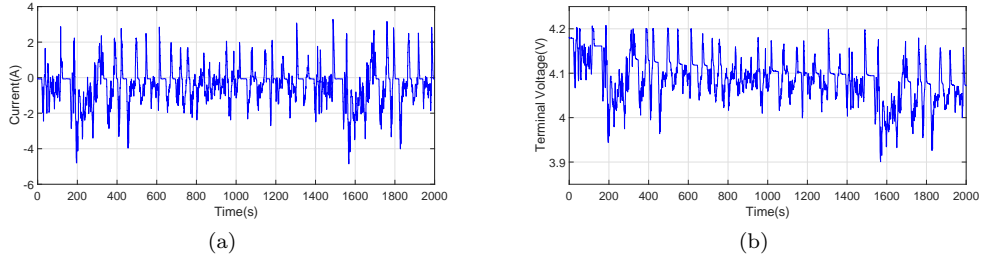


Figure 6. UDDS drive cycle. (a) Discharging current. (b) Terminal voltage.

Case 1: The Simulation Results with Uncorrelated Noises.

Let the covariances of the process and measurement noises be $Q_k = 10^{-14}I_8$ and $R_k = 10^{-6}$, respectively. Set other parameters as $\gamma_{1,k} = 0.3$, $\gamma_{2,k} = 3 \times 10^{-4}$ and $\Xi_{u,0|0} = 10^{-10}I_8$.

The comparison results under the pulse current test are shown in Fig. 7a. Moreover, the error curve between the true SOC and the estimated SOC is shown in Fig. 7b. Similarly, under the UDDS situation, the results are shown in Fig. 8.

From Figs. 7b and 8b, we can find that the error of our proposed SOC estimation scheme is much less than the standard EKF, which demonstrates the effectiveness of our proposed SOC estimation scheme.

Case 2: The Estimator With Correlated Noises.

The correlated noises are set as

$$\begin{aligned} w_k &= \alpha_k + \alpha_{k-1}, \\ v_k &= \beta_k + \beta_{k-1} \end{aligned}$$

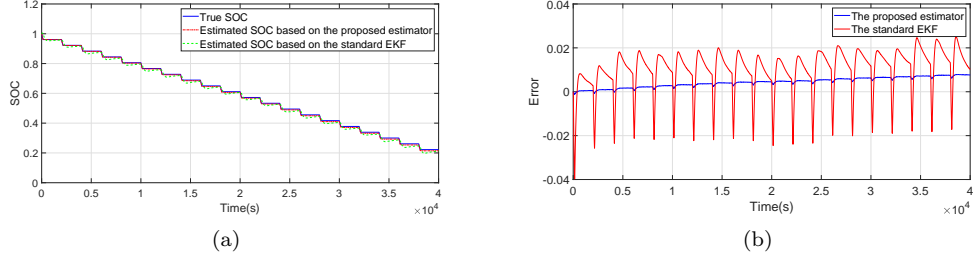


Figure 7. Pulse current test. (a) The comparison of actual SOC and estimated SOC. (b) The error of SOC.

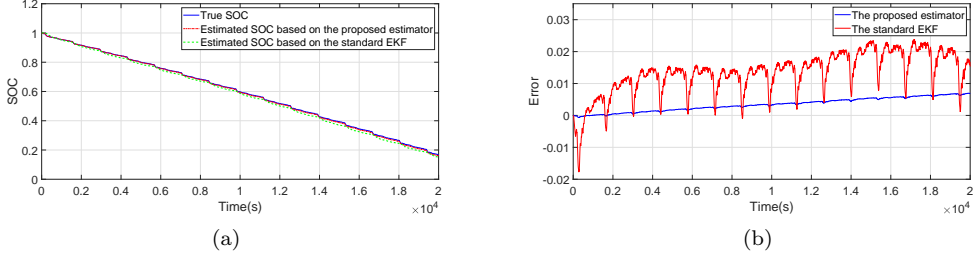


Figure 8. UDDS drive cycle. (a) The comparison of actual SOC and estimated SOC. (b) The error of SOC.

where α_k is a zero-mean Gaussian white noise with covariance Q_k and β_k is a zero-mean Gaussian white noise with covariance R_k .

We set $\gamma_{3,k} = 0.3$, $\gamma_{4,k} = 3 \times 10^{-4}$ and $\gamma_{5,k} = 10^{-3}$. The noise covariances Q_k and R_k are set as $10^{-12}I_8$ and 10^{-6} , respectively. The initial estimation error covariance is set as $\Xi_{c,0|0} = 10^{-10}I_8$.

The comparison results under the pulse current test are shown in Fig. 9a. Moreover, the error curve between the true SOC and the estimated SOC is shown in Fig. 9b. Similarly, under the UDDS situation, the results are shown in Fig. 10. From Figs. 9-

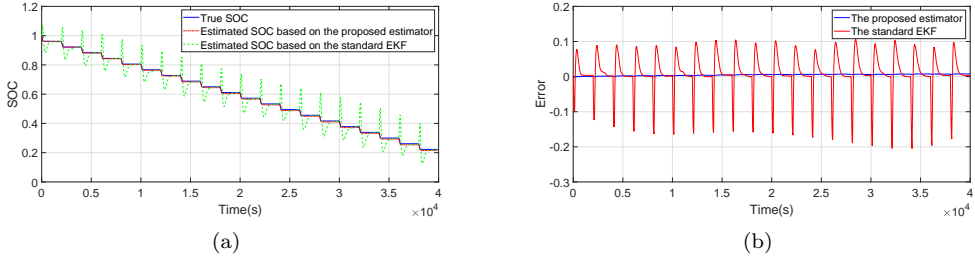


Figure 9. Pulse current test. (a) The comparison of actual SOC and estimated SOC. (b) The error of SOC.

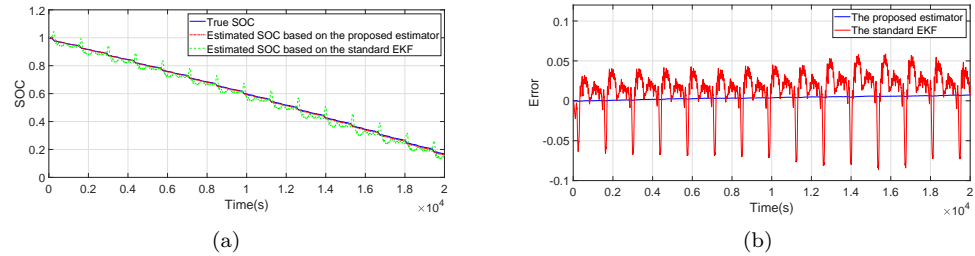


Figure 10. UDDS drive cycle. (a) The comparison of actual SOC and estimated SOC. (b) The error of SOC.

10, it can be seen that the proposed SOC estimation scheme performs well even in the presence of uncertain parameters and correlated noises.

5. Conclusion

In this paper, the SOC estimation problem for Li-ion batteries has been investigated. A model of Li-ion batteries with uncertain parameters has been established. The uncorrelated and correlated noises have been considered in the SOC estimator design, respectively. Based on the proposed SOC estimation scheme, the upper bound for the estimation error covariance has been derived. Then, such an upper bound is minimized by appropriately designing the estimator gain. Finally, simulation experiments for the SOC estimation have been carried out to verify the state estimator performance. The results show that the proposed estimator scheme performs better than the EKF in the presence of uncertain parameters and uncorrelated/correlated noises. In future work, we plan to identify a more accurate model to reduce the model error and extend some novel theoretical results to the SOC estimation problem.

Acknowledgements

The authors would like to express appreciation to the anonymous reviewers and Editors for their very helpful comments that improved the paper.

Disclosure statement

No potential conflict of interest was reported by the authors.

Funding

This project was funded by the Deanship of Scientific Research (DSR) at King Abdulaziz University, Jeddah, under grant no. (RG-7-135-41). The authors, therefore, acknowledge with thanks DSR for technical and financial support. This work is also supported in part by the Program of Shanghai Academic/Technology Research Leader [grant number 20XD1420100] and the Natural Science Foundation of Shanghai of China [grant number 18ZR1401500].

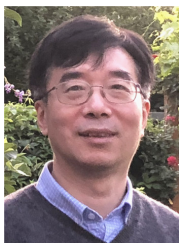
Notes on contributors



Junwei Wang received the B.Eng. degree in electrical engineering and automation from the University of Shanghai for Science and Technology, Shanghai, China, in 2018. She is currently pursuing the M.Eng. degree in control science and engineering at Donghua University, Shanghai, China. Her current research interests include battery modeling, stochastic control and filtering, as well as state estimation for electric drive vehicle applications.



Bo Shen received the B.Sc. degree in mathematics from Northwestern Polytechnical University, Xian, China, in 2003, and the Ph.D. degree in control theory and control engineering from Donghua University, Shanghai, China, in 2011. From 2009 to 2010, he was a Research Assistant with the Department of Electrical and Electronic Engineering, The University of Hong Kong, Hong Kong. From 2010 to 2011, he was a Visiting Ph.D. Student with the Department of Information Systems and Computing, Brunel University London, London, U.K. From 2011 to 2013, he was a Research Fellow (Scientific Co-Worker) with the Institute for Automatic Control and Complex Systems, University of Duisburg-Essen, Duisburg, Germany. He is currently a Professor with the College of Information Science and Technology, Donghua University. He has published around 80 articles in refereed international journals. His research interests include nonlinear control and filtering, stochastic control and filtering, as well as complex networks and neural networks. Prof. Shen is a program committee member for many international conferences. He serves (or has served) as an Associate Editor or Editorial Board Member for eight international journals, including *Systems Science and Control Engineering*, *Journal of The Franklin Institute*, *Asian Journal of Control*, *Circuits, Systems, and Signal Processing*, *Neurocomputing*, *Assembly Automation*, *Neural Processing Letters*, and *Mathematical Problems in Engineering*.



Zidong Wang was born in Jiangsu, China, in 1966. He received the B.Sc. degree in mathematics in 1986 from Suzhou University, Suzhou, China, and the M.Sc. degree in applied mathematics in 1990 and the Ph.D. degree in electrical engineering in 1994, both from Nanjing University of Science and Technology, Nanjing, China. He is currently a Professor of Dynamical Systems and Computing in the Department of Computer Science, Brunel University London, U.K. From 1990 to 2002, he held teaching and research appointments in universities in China, Germany and the UK. Prof. Wang's research interests include dynamical systems, signal processing, bioinformatics, control theory and applications. He has published around 600 papers in refereed international journals. He is a holder of the Alexander von Humboldt Research Fellowship of Germany, the JSPS Research Fellowship of Japan, William Mong Visiting Research Fellowship of Hong Kong. Prof. Wang serves (or has served) as the Editor-in-Chief for *Neurocomputing*, Deputy Editor-in-Chief for *International Journal of Systems Science*, and an Associate Editor for 12 international journals including *IEEE Transactions on Automatic Control*, *IEEE Transactions on Control Systems Technology*, *IEEE Transactions on Neural Networks*, *IEEE Transactions on Signal Processing*, and *IEEE Transactions on Systems, Man, and Cybernetics-Part C*. He is a Member of the *Academia Europaea*, a Fellow of the *IEEE*, a Fellow of the *Royal Statistical Society* and a member of program committee for many international conferences.



Fuad E. Alsaadi received the B.S. and M.Sc. degrees in electronic and communication from King AbdulAziz University, Jeddah, Saudi Arabia, in 1996 and 2002, respectively, and the Ph.D. degree in optical wireless communication systems from the University of Leeds, Leeds, U.K., in 2011. Between 1996 to 2005, he worked in Jeddah as a communication instructor with the College of Electronics and Communication. He is currently an Associate Professor of the Electrical and Computer Engineering Department within the Faculty of Engineering, King Abdulaziz University, Jeddah, Saudi Arabia. He has published widely in the top IEEE communications conferences and journals and has received the Carter Award from the

University of Leeds for the best Ph.D. His research interests include optical systems and networks, signal processing, synchronization, and systems design.



Khalid H. Alharbi received the Ph.D. degree in electrical engineering from the University of Glasgow of the UK in 2016. He is currently an Assistant Professor in the Department of Electrical and Computer Engineering at King Abdulaziz University. His research interest includes micro/nano-fabrication technologies, millimeter wave and THz antennas, and RTD-based devices.

References

- Andre, D., Meiler, M., Steiner, K., Walz, H., Soczka-Guth, T., & Sauer, D. U. (2011). Characterization of high-power lithium-ion batteries by electrochemical impedance spectroscopy. II. modelling. *Journal of Power Sources*, 196(12), 5349–5356.
- Burke, A. F. (2007). Batteries and ultracapacitors for electric, hybrid, and fuel cell vehicles. *In Proceedings of the IEEE*, 95(4), 806–820.
- Charkhgard, M., & Farrokhi, M. (2010). State-of-charge estimation for lithium-ion batteries using neural networks and EKF. *IEEE Transactions on Industrial Electronics*, 57(12), 4178–4187.
- Chemali, E., Kollmeyer, P., Preindl, M & Emadi, A. (2018). State-of-charge estimation of Li-ion batteries using deep neural networks: A machine learning approach. *Journal of Power Sources*, 400, 242–255.
- Chen, Z., Fu, Y., & Mi, C. C. (2013). State of charge estimation of Lithium-ion batteries in electric drive vehicles using extended Kalman filtering. *IEEE Transactions on Vehicular Technology*, 62(3), 1020–1030.
- Cheng, M. W., Lee, Y. S., Liu, M., & Sun, C. C. (2015). State-of-charge estimation with aging effect and correction for lithium-ion battery. *IET Electrical System in Transportation*, 5(2), 70–76.
- Feng, J., Wang, Z., & Zeng, M. (2011). Optimal robust non-fragile Kalman-type recursive filtering with finite-step autocorrelated noises and multiple packet dropouts. *Aerospace Science & Technology*, 15(6), 486–494.
- Feng, J., Wang, Z., & Zeng, M. (2013). Distributed weighted robust Kalman filter fusion for uncertain systems with autocorrelated and cross-correlated noises. *Information Fusion*, 14(1), 78–86.
- Fu, A., & Song, E. (2008). The optimal Kalman type state estimator with multi-step correlated process and measurement noises. *In Proceedings of the International Conference on Embedded Software & Systems*, (pp. 215–220).
- Gao, J., Zhang, Y., & He, H. (2015). A real-time joint estimator for model parameters and state of charge of Lithium-ion batteries in electric vehicles. *Energies*, 8(8), 8594–8612.
- He, Y., Liu, X., Zhang, C., & Chen, Z. (2013). A new model for state-of-charge (SOC) estimation for high-power Li-ion batteries. *Applied Energy*, 101, 808–814.
- He, Z., Chen, D., Pan, C., Chen, L., & Wang, S. (2016). State of charge estimation of power Li-ion batteries using a hybrid estimation algorithm based on UKF. *Electrochimica Acta*, 211, 101–109.
- Hu, J., Wang, Z., & Gao, H. (2013). Recursive filtering with random parameter matrices, multiple fading measurements and correlated noises. *Automatica*, 49(11), 3440–3448.
- Hu, J., Wang, Z., Liu, G., Jia, C & Williams, J. (2020). Event-triggered recursive state estimation for dynamical networks under randomly switching topologies and multiple missing measurements. *Automatica*, 115.
- Jeong, Y. M., Cho, Y. K., Ahn, J. H, Ryu, S. H., & Lee, B. K. (2014). Enhanced Coulomb counting method with adaptive SOC reset time for estimating OCV. *In Proceedings of the IEEE energy conversion Congress and Exposition*, (pp. 4313–4318).

- Johnson, V. H., Pesaran, A. A., & Sack, T. (2001). Temperature-dependent battery models for high-power Lithium-ion batteries. *In Proceedings of the Annual Electric Vehicle Symposium*, (pp. 1–14).
- Khaligh, A., & Li, Z. (2010). Battery, ultracapacitor, fuel cell, and hybrid energy storage systems for electric, hybrid electric, fuel cell, and plug-in hybrid electric vehicles: state of the art. *IEEE Transactions on Vehicular Technology*, *59*(6), 2806–2814.
- Kim, T., Song, W., Son, D., Ono, L., & Qi, Y. (2019). Lithium-ion batteries: outlook on present, future, and hybridized technologies. *Journal of Materials Chemistry A*, *7*(7), 2942–2964.
- Kollmeyer, P., Hackl, A., & Emadi, A. (2017). Li-ion battery model performance for automotive drive cycles with current pulse and EIS parameterization. *In Proceedings of the IEEE Transportation Electrification Conference and Expo*, (pp. 486–492).
- Kollmeyer, P. (2018). Panasonic 18650PF Li-ion Battery Data. <https://doi.org/10.17632/wykht8y7tg.1>.
- Li, X. (2003). Optimal linear estimation fusion, Part VII: Dynamic systems, *In Proceedings of the Sixth International Conference of Information Fusion*, (pp. 455–462).
- Li, X., Han, F., Hou, N., Dong, H., & Liu, H. (2020). Set-membership filtering for piecewise linear systems with censored measurements under Round-Robin protocol. *International Journal of Systems Science*, *51*(9), 1578–1588.
- Luo, W., Lv, C., Wang, L., & Liu, C. (2011). Study on impedance model of Li-ion battery. *In Proceedings of the IEEE Conference on Industrial Electronics and Applications*, (pp. 1943–1947).
- Mastali, M., Vazquez-Arenas, J., Fraser, R., Fowler, M., Afshar, S., & Stevens, M. (2013). Battery state of the charge estimation using Kalman filtering. *Journal of Power Sources*, *239*, 294–307.
- Mauracher, P., & Karden, E. (1997). Dynamic modelling of Lead/Acid batteries using impedance spectroscopy for parameter identification. *Journal of Power Sources*, *67*, 69–84.
- Meng, J., Luo, G., & Gao, F. (2016). Lithium polymer battery state-of-charge estimation based on adaptive unscented Kalman filter and support vector machine. *IEEE Transactions on Power Electronics*, *31*(3), 2226–2238.
- Pizarro-Carmona, V., Cortes-Carmona, M., Palma-Behnke, R., Calderon-Munoz, W., Orchard, M. E., & Estevez, P. A. (2019). An optimized impedance model for the estimation of the state-of-charge of a Li-ion cell: the case of a LiFePO₄ (ANR26650). *Energies*, *12*(4), 1–16.
- Plett, G. L. (2006). Sigma-point Kalman filtering for battery management systems of LiPB-based HEV battery packs. Part 1: Introduction and state estimation. *Journal of Power Sources*, *161*(2), 1356–1368.
- Qu, B., Li, N., Liu, Y., & Alsaadi, F. E. (2020). Estimation for power quality disturbances with multiplicative noises and correlated noises: a recursive estimation approach. *International Journal of System Science*, *51*(7), 1200–1217.
- Santhanagopalan, S., & White, R. E. (2006). Online estimation of the state of charge of a lithium ion cell. *Journal of Power Sources*, *161*(2), 1346–1355.
- Schweighofer, B., Wegleiter, H., Recheis, M., & Fulmek, P. (2012). Fast and accurate battery model applicable for EV and HEV simulation. *In Proceedings of the IEEE International Instrumentation and Measurement Technology Conference*, (pp. 565–570).
- Song, J., Ding, D., Liu, Y., & Wang, X. (2020). Non-fragile distributed state estimation over sensor networks subject to DoS attacks: the almost sure stability. *International Journal of Systems Science*, *51*(6), 1119–1132.
- Song, E., Zhu, Y., Zhou, J., & You, Z. (2007). Optimal Kalman filtering fusion with cross-correlated sensor noises. *Automatica*, *43*(3), 1450–1456.
- Tan, H., Shen, B., Peng, K., & Liu, H. (2020). Robust recursive filtering for uncertain stochastic systems with amplify-and-forward relays. *International Journal of Systems Science*, *51*(7), 1188–1199.
- Xing, Y., He, W., Pecht, M., & Kwok, T. (2014). State of charge estimation of lithium-ion batteries using the open-circuit voltage at various ambient temperatures. *Applied Energy*, *113*, 106–115.

- Xiong, R., Cao, J., Yu, Q., He, H., & Sun, F. (2018). Critical review on the battery state of charge estimation methods for electric vehicles. *IEEE Access*, *6*, 1832–1843.
- Yang, N., Zhang, X., & Li, G. (2015). State of charge estimation for pulse discharge of a LiFePO₄ battery by a revised ah counting. *Electrochimica Acta*, *151*, 63–71.
- Zhang, H., Hu, J., Liu, H., Yu, X & Liu, F. (2019). Recursive state estimation for time-varying complex networks subject to missing measurements and stochastic inner coupling under random access protocol. *neurocomputing*, *346*. 48–57.
- Zhang, L., Hu, X., Wang, Z., Sun, F.,& Dorrell, D. G. (2018). A review of supercapacitor modeling, estimation, and applications: a control/management perspective. *Renewable & Sustainable Energy Reviews*, *81*, 1868–1878.